JOURNAL OF APPLIED ELECTROCHEMISTRY 17 (1987) 613–624

Photoelectrochemical properties of p-RuS_2

S. PIAZZA*, H. TRIBUTSCH

Hahn-Meitner-Institut für Kernforschung Berlin, Bereich Strahlenchemie, D-1000 Berlin 39, Federal Republic of Germany

Received 29 March 1986; revised 8 July 1986

An impedance study of the *p*-RuS_2/aqueous electrolyte interface confirms the existence of a Fermi level pinning of the semiconductor. The mechanisms of the band shift and of the interaction with a redox couple are illustrated. The photopotential is limited by the moderate quality of the barrier which allows forward currents flowing through the interface.

The effect of the interface modification by means of a metal deposition on the semiconductor surface has been investigated. An improvement in the catalysis with respect to both photoassisted hydrogen evolution and oxygen dark reduction was found. Evidence for an insertion of hydrogen into p-RuS_2 is also presented.

1. Introduction

RuS_2 (E_g = 1.3 eV) is an interesting material due to the possible catalytic properties of ruthenium-containing compounds. n-Type RuS_2 crystals recently investigated [1–8] showed a remarkable chemical stability [9, 10]. In particular they are resistant to all common chemical etchings and are stable during strong oxygen evolution.

p-Type RuS_2 has been grown [11] to test the stability of the crystals under hydrogen evolution and to check the catalytic properties of this material toward oxygen reduction. The photoelectrochemical investigation on these crystals revealed an anomalous behaviour of the *p*-RuS_2/aqueous electrolyte interface [11]. Moreover, the presence of forward currents indicated a moderate quality of the Schottky barrier, despite sensible photopotential values (up to 0.45 V) recorded at high levels of illumination. Further investigation on these aspects is reported in the present paper.

Metal deposition on the semiconductor surface was also performed. The aim was to improve catalysis toward photoassisted hydrogen evolution according to previous results on different materials [12–15]. In the case of *p*-RuS_2 crystals, however, special interest arises from the good stability of the material under highly reductive operating conditions [11, 16].

Oxygen reduction occurs on RuS_2 crystals both in acidic and basic solutions with slow kinetics [11]. The behaviour of the modified electrodes in this regard is also briefly discussed.

2. Experimental details

RuS_2 crystals were grown in molten bismuth [9, 10]. To obtain a *p*-type conductivity, $RuAs_2$ and FeS_2 were added as dopants before the crystal growth. The preparation procedure is described in detail elsewhere [10, 11]. Crystals were mounted on Vespel holders and sealed with an epoxy resin (Scotchcast 3M XR 5241) leaving only one surface in contact with the solution (typical surface area of about 1 mm^2). Electrical back contacts were ensured by means of a platinum drop.

The experimental set-up consisted of a potentiostat-sweep generator (BANK, POS 73), a lock-in amplifier (PAR, Mod. 124A or 5206) and a X–Y–t recorder. The impedance measurements were performed using the lock-in technique: an a.c. signal, having 10 mV peak-to-peak amplitude and different frequencies (see below), modulated the electrode potential. The out-of- phase component of the a.c. current was calibrated by means of a decade capacitor (Hewlett–Packard 4440B), the in-phase component by means of a resistance box (Monacor RD-1000).

**Present address*: Istituto di Ingegneria Chimica, Universita di Palermo, Viale delle Scienze, 90128 Palermo, Italy.

0021–891X/87 $03.00 + .12

For the light modulated induced electron resonance (LMIER) measurements [17] an inductance, $L = 280\,\text{mH}$, was added in series with the cell and, for any electrode potential, forced photocurrent oscillations were induced by illuminating the electrode with a chopped white light. The light source was a 250-W W-Hal lamp (Oriel) and the photocurrent oscillations were monitored using an oscilloscope. The frequency of the chopper (PAR 9479) was varied until electrical resonance was achieved in the RLC circuit.

A standard three-electrode cell was used with platinum as the counterelectrode and a mercurous sulphate electrode (MSE) as a reference. Solutions were made using analytical-grade reagents and triply distilled water. Experiments were carried out at room temperature and without bubbling gas through the electrolyte unless specified.

The deposition of metals on p-RuS_2 was carried out with illumination of the semiconductor surface in aqueous solutions containing 10^{-3} M $RuCl_3$, $RhCl_3 \cdot xH_2O$ or $PtCl_2$ in 3 M HCl. In the last case a continuously stirred suspension was obtained, due to the very slight solubility of the salt. During deposition the electrode potential was scanned at $100\,\text{mV}\,\text{s}^{-1}$, first between -0.5 and -0.2 V (MSE) for some minutes and then between -1.1 and -0.6 V (MSE) for 1 h. During the deposition the dark currents increased. The electrodes were then etched in concentrated HCl until the dark current was reduced, and were then rinsed with distilled water. Finally, cyclic voltammetry was carried out in 0.5 M H_2SO_4 solution under illumination between -0.65 and 0.5 V (MSE) for some hours. This procedure gave good results and stability of the metal deposit, at least for the case of platinum (see Results section).

The analysis of the surfaces was performed by means of a scanning electron microscope (Cambridge Instruments).

3. Results and discussion

3.1. *Capacitance measurements*

An earlier study performed on the p-RuS_2/aqueous electrolyte interface [11] has shown that the band edges of the semiconductor are shifted with the redox level of the electrolyte. This is in agreement with analogous findings on n-type crystals grown in molten bismuth [9], and was attributed to the presence on the semiconductor surface of a high number of surface states. To detect the energy position of the semiconductor bands capacitance measurements were performed in the dark in aqueous solutions containing different redox couples. The results of these measurements were complicated by the moderate blocking character of the barrier, which allows remarkable dark current to cross the interface. Moreover, the crystal surface generally presented quite irregular features and the quality of the investigated crystals was not uniform. Due to all these facts the results varied from crystal to crystal. Nevertheless, the systematic investigation of many crystals under different experimental conditions allowed the detection of some features which are common to all the cases examined.

Going from anodic to cathodic electrode potentials the capacitance curve presents no monotonic parts until the proximity of the redox potential of the solution is reached. In this region a monotonic decrease of the capacitance was recorded at all the investigated frequencies (100 Hz to 2 kHz). The value of the capacity, C, of the system decreased with increase of the frequency. In the absence of additional redox couples the monotonic part was observed in the region of hydrogen evolution.

The equivalent electrical circuit of the electrochemical cell can be schematized with two capacities in series: that of the semiconductor space charge region, C_{sc}, and that of the

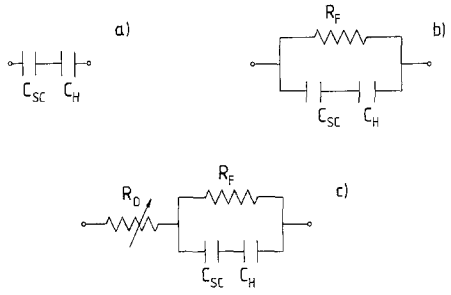

Fig. 1. Electrical equivalent circuits of the crystalline semiconductor–electrolyte junction, (a) in the absence and (b) in the presence of a faradic dark current, and (c) in the presence of a variable series resistance.

Helmholtz layer, C_H (Fig. 1a). The former of these is a function of the applied potential. If the band edges of the semiconductor are fixed, the usual Mott–Schottky approximation [18, 19] holds in the frequency range in which surface states are 'switched off'. The second capacitance is a constant: a typical value assumed for aqueous solutions is 20 μF cm^{-2} [20]. In the present case, due to the faradic currents crossing the interface, a faradic resistence in parallel to the capacities must be added as in Fig. 1b [21, 22]. In this case it is necessary to calculate the parallel capacitance of the circuit given by

$$C_p = \frac{1}{2\pi f|Z|} \sin \delta \qquad (1)$$

where f is the frequency, δ is the phase angle and Z the complex impedance of the system

$$Z = X + iY \qquad (2)$$

In the present case, however, the imaginary part of the impedance was always much higher than the real part. This led to corrections of the order of the experimental error ($< 3\%$) and they were generally neglected.

The Mott–Schottky plots calculated for all solutions showed a straight-line behaviour only in a region of the monotonic part of the capacitance curve. The width of this linear region was normally 150–300 mV depending on the electrode and, to a certain extent, also on the solution. In particular, it was observed that with electrodes allowing lower faradaic currents the linear region was wider. Moreover, a very strong frequency dispersion was observed, as shown in Fig. 2, in which C^{-2} versus U_E plots are shown at different frequencies. Nevertheless, all these straight lines converged to about the same point on the x-axis for all crystals, regardless of their quality. For example, in 1 N H_2SO_4 solution it was possible to estimate an apparent flat band potential value of 0.97 $\pm$ 0.06 V (MSE). Analogous behaviour was recorded in the presence of additional redox couples, but the linear Mott–Schottky plots, and hence the apparent flat band potentials, V_{FB}^{app}, were shifted according to the redox potential of the solution (see below). The reproducibility of the V_{FB}^{app} values was often better in the presence of a redox couple.

Frequency dispersion in the capacity measurements has often been observed in the literature [21]. Possible causes are:

(a) contribution of the bulk of the electrode or of the back contact to the overall impedance;

(b) non-uniform a.c. current distribution due to irregularity of the electrode surface;

(c) partial contribution of surface states to the capacitance response.

All these causes could contribute to the observed frequency dispersion in the present case (for example, the electrode surface often presented remarkably high roughness). However, for the investigated p-RuS_2 crystals the frequency dispersion is quite high (see Fig. 2). For this reason the possible influence of relaxation phenomena caused by polar double-layer constituents [23] leading to a much slower frequency dependence was discarded as a principal cause. On the contrary, it was shown [24] that the presence of surface states having a continuous energy distribution in the forbidden gap of the semiconductor can cause a linear relationship between C^{-2} and f.

The dependence of the Mott–Schottky curves and of V_{FB}^{app} on the pH of the solution, in the

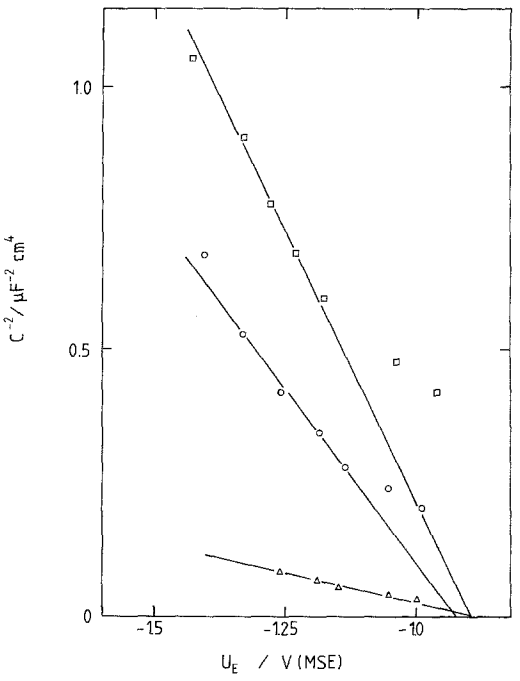

Fig. 2. Mott–Schottky plots at different frequencies for a p-RuS_2 electrode in 0.5 M H_2SO_4 solution. □, f = 2 kHz; ○, f = 1 kHz; △, f = 300 Hz.

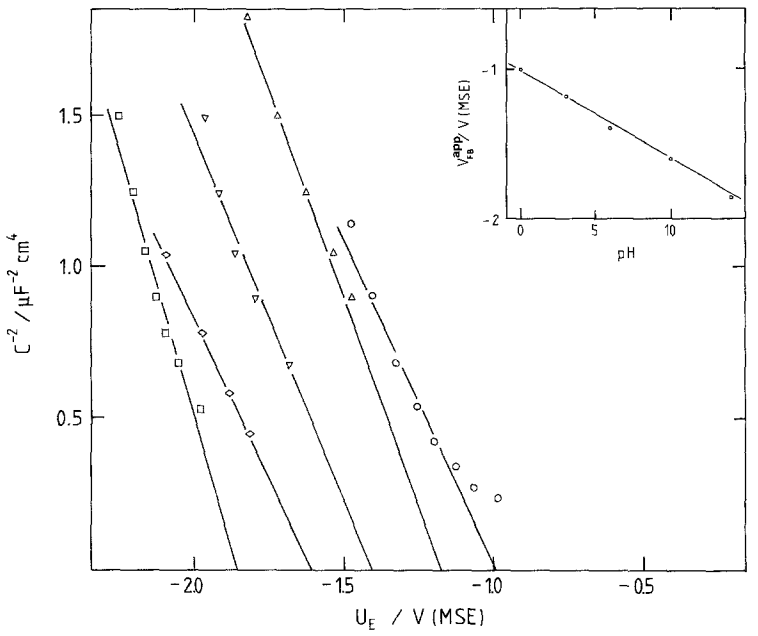

Fig. 3. Dependence of the Mott–Schottky lines on pH at f = 1 kHz in aqueous solutions containing no additional redox couples. ○, pH = 0; △, pH = 3; ▽, pH = 6; ◇, pH = 10; □, pH = 14. The shift of the apparent flat band potential with pH is represented in the inset.

absence of any additional redox couple, is shown in Fig. 3. The apparent flat band potential is shifted about 60 mV per unit of pH. This fact is related more to the shift of hydrogen evolution in the dark than to an ionic adsorption or to an acid–base equilibrium with an oxide layer. It is worth noting that the Mott–Schottky lines at different pHs are not parallel. Typically, the variation of the slopes is within a factor of two: in Fig. 3 the values range between about 2.5 and 5 $\mu F^{-2} cm^4 V^{-1}$. The slope of the Mott–Schottky lines for the same electrode was also found to be slightly dependent on the redox couple present in solution at pH = 0. This behaviour was also observed for n-type RuS_2 crystals (see Fig. 6 in [9]), and together with the previous considerations (see Figs 2, 3) indicates that the recorded slopes do not reflect the properties of the space charge region (i.e. the concentration of free carriers). Nevertheless, as already observed in many cases in the literature [21, 23], a Mott–Schottky-like relationship between the capacity of the system and the electrode potential holds, giving an indication of the position of the band edges. Again, a proportionality between C^{-2} and V can be valid under less restrictive conditions than those of the ideal case [25].

By changing the redox species in solution at

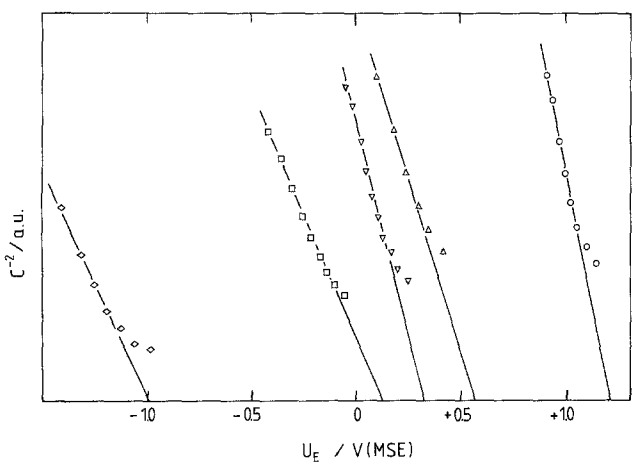

Fig. 4. Mott–Schottky plots recorded at pH = 0 and f = 1 kHz in the presence of different redox species. ○, 0.4 M Ce^{4+} (or Ce^{4+}/Ce^{3+}); △, 0.5 M Fe^{3+}/Fe^{2+}; ▽, 0.1 M Ru^{3+}; □, 0.5 M Cu^{2+}. For comparison, the curve obtained without additional redox couples (◇) is also reported.

pH = 0 the Mott–Schottky straight lines are displaced more than 2 V according to the redox level of the electrolyte (Fig. 4). Moreover, a difference was noted in many cases between solutions containing both forms of the redox couple and those containing only oxidized species. The results shown in Fig. 4 are in agreement with the reported shift of the photocurrent onset with the redox potential of the electrolyte [11]. It is confirmed that such a shift occurs in the dark due to a Fermi level pinning by surface states.

3.2. *Photoelectrochemical behaviour*

An attempt was made to correlate the apparent flat band potential extrapolated from the Mott–Schottky plots to the potential of photocurrent onset. Some results are summarized in Table 1, in which the potential at which the cathodic dark current begins is also given. In Table 1 it is possible to distinguish between the last three cases and the others. In the last three solutions the redox level is well determined due to the presence of both forms of the redox couple (for solutions with added Ce^{4+} ions relevant quantities of Ce^{3+} are always present because of the very oxidative character of these ions), or to the solubility product of one form of the couple. Under these circumstances V_{FB}^{app} in the dark is nearly coincident with the onset of photocurrent. This finding can be explained according to the scheme shown in Fig. 5. Applying an anodic potential a forward anodic dark current is observed (see curve b of Fig. 6), caused by the hopping of holes from the valence band through the barrier. A negative change in the electrode potential causes an upward shift of the band edges due to the filling of surface states (Fig. 5a). Under illumination a cathodic photocurrent begins when the redox level of the solution, E_{red}, is lower than the quasi-Fermi level of the electrons, $^*E_{F,n}$ (Fig. 5b), i.e. in the domain of the anodic dark current, as experimentally observed. The shift of the bands in the dark continues, and at $U_E = E_{red}$ the sign of the dark current is reversed (compare Figs 5 and 6). In this region of potential the position of the band edges becomes fixed due to an interaction between surface states and the redox couple [26, 27]. The band bending now increases according to the imposed variations of potential, and the surface states remain in equilibrium with the solution (Fig. 5d). From this point a Mott–Schottky straight line is recorded. The difference between this point and the apparent flat band potential is given approximately by the barrier height, and is nearly equal to the photopotential recorded at high illumination levels. For this reason $V_{Fb}^{app} = V_{onset}$.

In the presence of the oxidized form of the couple only, the kinetic interaction between surface states and the redox couple is less effective. The shift of the bands continues for some hundreds of mV until some quantity of the reduced species is formed in the dark (see Table 1). This shift is reflected by the different shape of the dark cathodic current curves a and c in comparison to curve b of Fig. 6 (the anodic currents are obviously suppressed in the absence of hole acceptors).

As for the small linearity range of the Mott–Schottky plots, it was observed that:

Table 1. Characteristic voltages for p-RuS_2 *in different electrolytes.* V_{cc} *is the potential at which cathodic dark current begins,* V_{onset} *is the photocurrent onset potential. With the exception of the first two, the solutions were obtained by adding the ions (as sulphate or chloride salts) to the base solution at pH = 0*

Solution	V_{cc} *(V vs MSE)*	V_{onset} *(V vs MSE)*	V_{FB}^{app} *(V vs MSE)*	$\lvert V_{FB}^{app}\rvert - \lvert V_{onset}\rvert$ *(V)*
H_2SO_4, 0.5M	−0.8	−0.35	~ −1.0	~ +0.65
KOH, 1 M	−1.55	−1.1	~ −1.85	~ +0.75
Fe^{3+}, 0.5–4 M	+0.15	+0.55	+0.20	−0.35
Ru^{3+}, 0.1 M	+0.2	+0.55	+0.31	−0.24
Cu^{2+}, 0.5 M	−0.25	+0.16	+0.12	−0.04
Fe^{3+}/Fe^{2+}, 0.5 M	0	+0.55	+0.56	+0.01
Ce^{4+}, 0.4 M[a]	+0.8	~ +1.25	+1.2	~ −0.05

[a] Or Ce^{4+}/Ce^{3+} solution.

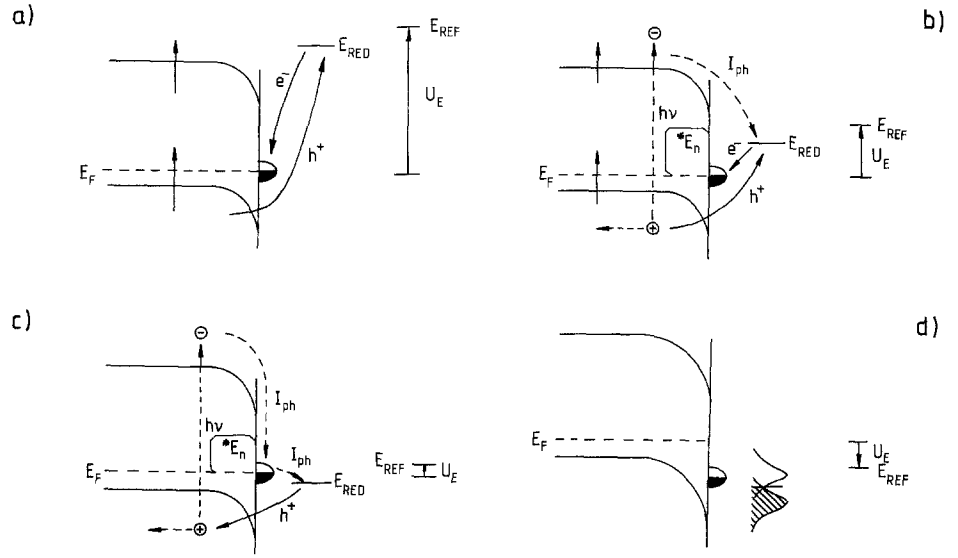

Fig. 5. Mechanisms of dark and photocurrent for p-RuS_2 in contact with an aqueous electrolyte at different electrode polarizations. For explanation see text.

(a) by lowering the concentration of oxidized species the linear region was decreased; at low concentrations the capacitance curve was deformed and tended to become flat (any influence of the Gouy layer is excluded due to the presence of 1 mol l^{-1} of H^+ ions);

(b) by stirring the solution the linear region of the Mott–Schottky plots was enlarged;

(c) on recently grown crystals which allow lower dark currents, the linearity of the Mott–Schottky plots is extended over more than 0.5 V (see Fig. 7). Moreover, these crystals showed the same behaviour reported in Fig. 4 and a lower frequency dispersion.

All these facts seem to indicate an influence of the diffusion of the oxidized species in solution reacting at the surface. When going towards negative potentials, cathodic currents increase until the concentration of the reacting species at the electrode surface is diffusion-limited. This fact can be taken into account by means of a series resistance varying with the potential (Fig. 1c). An analysis of the dependence of the imaginary part on the real part of the equivalent impedance is shown in Fig. 8. At less negative potentials the results are consistent with the scheme of Fig. 1a, whilst at more negative potentials they indicate the equivalent circuit shown in Fig. 1c [28]. However, a contribution of the bulk of the electrode to the series resistance cannot be

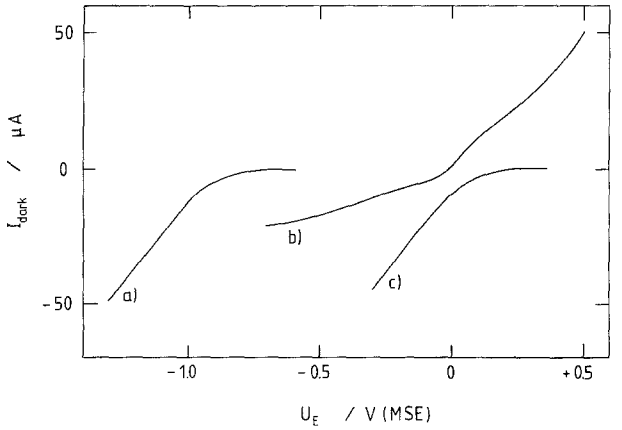

Fig. 6. Dark current as a function of the electrode potential for a p-RuS_2 electrode in different solutions. (a) 0.5 M H_2SO_4; (b) 0.5 M H_2SO_4 + 0.5 M $FeSO_4$ + 0.25 M $Fe_2(SO_4)_3$; (c) 0.5 M H_2SO_4 + 0.25 M $Fe_2(SO_4)_3$.

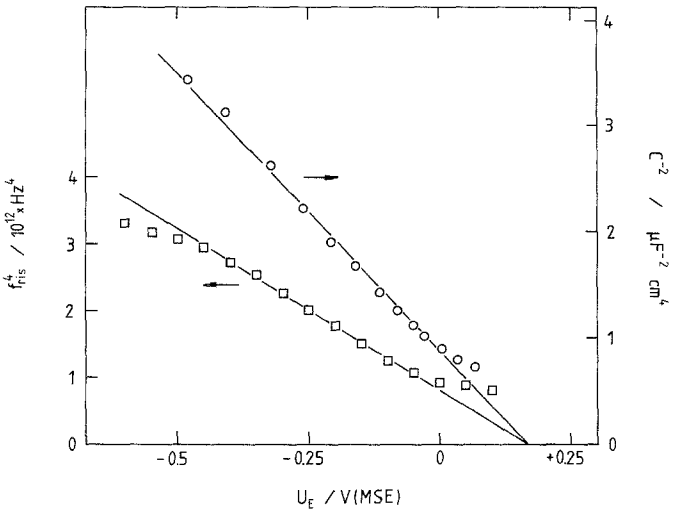

Fig. 7. Determination of the apparent flat band potential with the LMIER method (squares) and with the lock-in technique at 1 kHz (circles, for p-Rus_2 in 0.5 M H_2SO_4 + 0.5 M $Fe_2(SO_4)_3$.

excluded. An influence of the diffusion phenomenon on the recorded Mott–Schottky plots has been found also for n-RuS_2 [9]. The physical reason may be the fact that the presence of the couple at the electrode surface is necessary to neutralize kinetically the surface states and hence to stabilize the position of the semiconductor band edges.

To check whether the measured capacities reflect the variations in the band bending of the semiconductor a LMIER measurement was performed [17, 29]. With this method, photocurrent transients, which depend on the capacitance of the semiconductor space charge region, are influenced by means of an external inductance (see Experimental section). Varying the frequency of the chopped light a resonance is achieved in the RLC circuit. It is possible to demonstrate that the resonance frequency, f_{res}, is inversely proportional to the square root of the capacity [17, 29]. Indeed, a straight line was observed in the f_{res}^4 versus U_E plot (Fig. 7). The agreement between the V_{FB}^{app} values detected with the two different methods is evident.

An interesting experimental finding is the linear dependence of the open circuit potential, ΔV_{ph}, on the light intensity (Fig. 9). The same result was found in solutions containing Cu^{2+} or $Fe(CN)_6^{3-}$ ions under white light, and also for n-type crystals under monochromatic irradiation in the presence of different redox couples [10].

This behaviour can be qualitatively explained as follows. In the presence of a forward dark current the total current under illumination is the difference between the photocurrent and the forward current. At the open circuit potential [30, 31],

$$i_{ph} = i_f \tag{3}$$

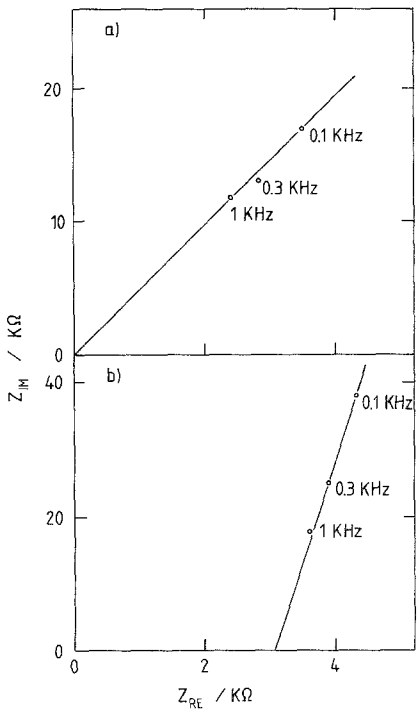

Fig. 8. Imaginary part versus real part of the electrode impedance at different frequencies for the electrode of Fig. 7. (a) $U_E = -0.1$ V (MSE); (b) $U_E = -0.6$ V (MSE).

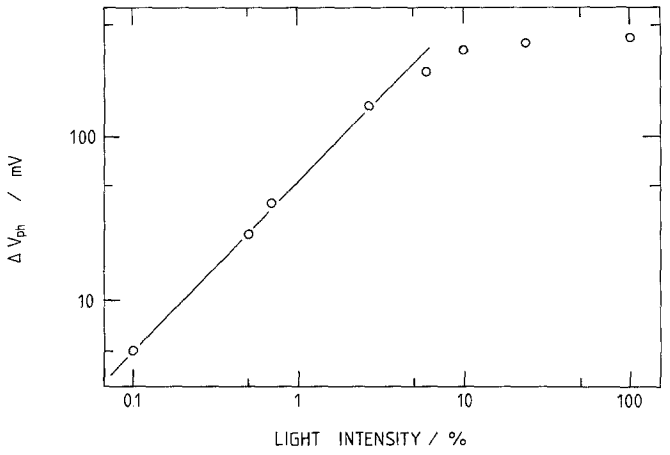

Fig. 9. Dependence of the open circuit photopotential on the white light intensity (expressed as percentage of the full irradiation power corresponding to about $2\,W\,cm^{-2}$) for p-RuS_2 in $0.5\,M$ H_2SO_4 + $0.5\,M$ $Fe_2(SO_4)_3$ solution.

For a hopping mechanism through traps lying inside the band gap it is possible to suppose [32], at least near the open circuit potential, that

$$i_f = K\Delta V \qquad (4)$$

where K is a proportionality constant and ΔV the voltage drop inside the semiconductor space charge layer (see also Fig. 6). In contrast, the potential dependence of the photocurrent has been experimentally found to be very weak in this potential region. This could be caused by the shift of the bands and/or by a high surface recombination rate. Recalling that in the considered range i_{ph} is proportional to the light intensity [11], the result of Fig. 9 is explained.

3.3. *Surface modification*

Deposition of platinum particles on the surface of p-RuS_2 semiconductors was carried out by electrochemical deposition from an electrolytic solution containing a platinum salt (see Experimental section for details). A partial coverage of the surface was obtained, as revealed by the SEM pictures of Fig. 10a and b. The platinum particles (bright areas) are not homogeneously distributed over the surface: large areas of uncovered surface are present, together with zones in which a high concentration of platinum is deposited, especially in coincidence with defects or irregularities of the surface (Fig. 10a). Moreover, the platinum particles appear to be rather small in size (Fig. 10b). From the inspection of the overall surface, and from a semiquantitative analysis, the degree of surface coverage was estimated to be lower than 20%.

From an electrical point of view the semiconductor–electrolyte junction is in parallel with a

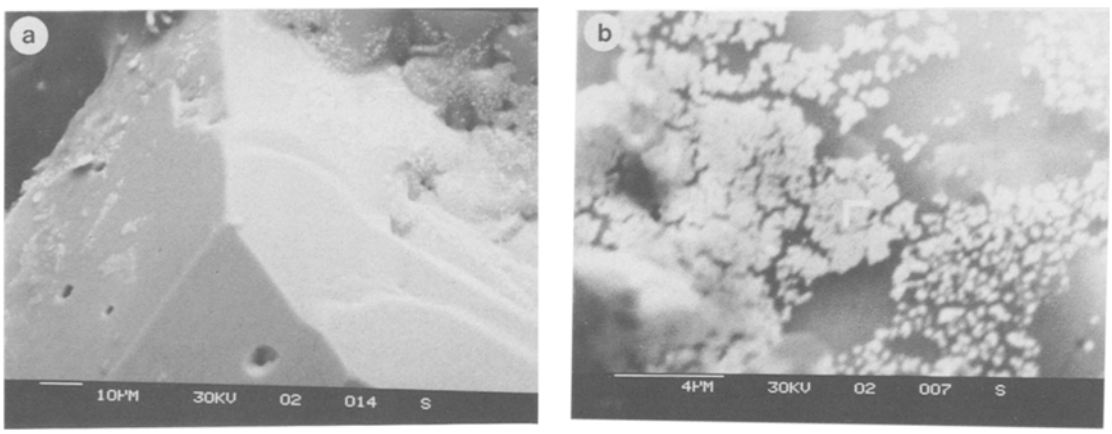

Fig. 10. (a) SEM micrograph of a p-RuS_2 crystal after electrochemical deposition of platinum (bright area). (b) Enlarged view of a platinum-rich area.

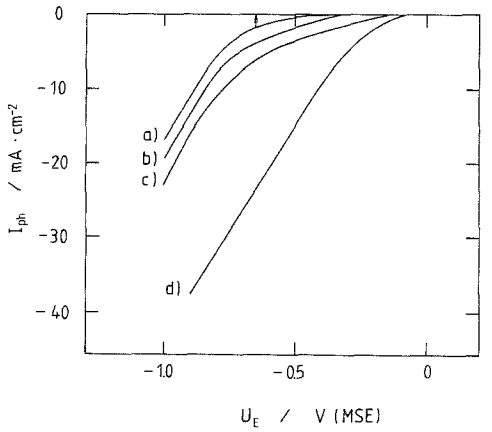

Fig. 11. Hydrogen evolution photocurrent versus electrode potential in 0.5 M H_2SO_4 under strong white light irradiation for the electrode of Fig. 10, before (a) and after (b, c) successive platinum electrodepositions and subsequent potential sweeps (d; see Experimental section).

semiconductor–metal–electrolyte junction. The voltage drop across the interface is determined by the lowest of the two barriers.

An effect on the photoassisted evolution of hydrogen was observed after this modification. Fig. 11 shows the variation of the photocurrent curve for hydrogen evolution in 0.5 M H_2SO_4 for the same electrode, before and after electrodeposition of platinum. The dark current (not considered in Fig. 11) increases by a factor of about two between curves a and d of Fig. 11, and is much lower than the photocurrent. It is interesting to note also the positive shift of the onset potential for hydrogen photoevolution. The calculated energy conversion for the incident light is, however, very low (less than 1%). Nevertheless, the result confirms that it is possible to improve the catalytic properties of the present system with this method.

Electrodeposition of rhodium and ruthenium was also carried out on the surface using the same procedure. In comparing the results, the fact that different crystals were used must be taken into account. Nevertheless, the effectiveness in improving the catalysis decreases in the order: platinum > rhodium > ruthenium (for ruthenium the photocurrent curve is displaced by about 100 mV). Moreover, with rhodium and ruthenium the dark current was more enhanced (perhaps due to a higher coverage of the surface). Therefore, it appears that the effect of the metal is a catalytic one, according to the results obtained on p-InP [15]. In the case of a p-type semiconductor, an increase of the Schottky barrier due to a semiconductor–metal contact should be inversely proportional to the work function of the metal. On the contrary, for p-RuS_2 the shift of the onset potential for hydrogen photoevolution seems to be related to the logarithm of the exchange current density for hydrogen dark evolution on the metal, $i_{O,H}$ [33].

This is confirmed by the oxygen reduction behaviour shown by the same crystal of Fig. 11. A noticeable increase in the rate of oxygen reduction on the electrode was found after platinum deposition. A comparison with an electrode without platinum on the surface is shown in Fig. 12 for the case of NaOH solution (the electrodes area is different in both cases). Limiting current is reached at a potential 450–500 mV more negative than the standard potential of the reaction (showed by an arrow in Fig. 12). The increase in the reduction kinetics is evident: for curve 1 of Fig. 12 the limiting current, i_L, is never reached until hydrogen evolution begins. The i_L values are obviously influenced by the bubbling rate, which causes stirring of the solution. For comparison, the behaviour of a platinum electrode was studied in the same conditions. The diffusion-limited current is reached at nearly the

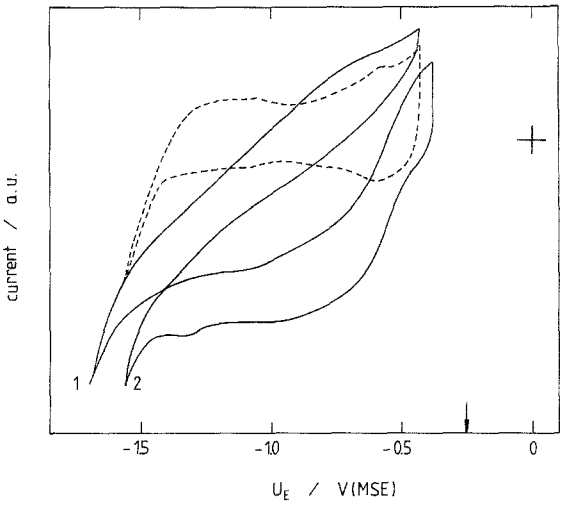

Fig. 12. Full lines: cyclic voltammetries performed on p-RuS_2 crystals in 1 M NaOH solution under oxygen atmosphere. Curve 1 refers to a crystal without platinum coverage; curve 2 is relative to the crystal of Fig. 10. Dashed curve is the voltammetry under nitrogen atmosphere corresponding to curve 2. Sweep rate, 100 mV s^{-1}.

same potential. The magnitude of i_L is equal in both cases if the apparent area of the electrodes are considered (in the case of the RuS_2 crystal, however, a roughness factor of 2.5 was calculated). This value is in agreement with those reported in the literature [34, 35]. Moreover, no effect of the semiconductor illumination on the potential at which limiting current is reached was found. This confirms that the effect of platinum on p-RuS_2 is mainly to improve the dark catalysis.

In sulphuric acid solutions the limiting current is reached at much higher overvoltages, not far from the hydrogen evolution starting potential.

Finally it is remarkable that in the case of platinum electrodeposition good stability was observed after many measurements. This holds also for hydrogen evolution, indicating an acceptable cohesive interaction between metallic catalyst and semiconductor.

4. Evidence for hydrogen insertion

The flatband measurements have revealed a remarkable anomaly occurring in connection with proton reduction leading to hydrogen evolution. The photopotentials amounting up to 450 mV (positive sign) observed with p-RuS_2 in presence of different redox systems can only be explained when the flatband potential of the electrode is situated at a potential more positive than the redox potential of the electrolyte. This means that the negative bending of the energy bands necessary for the generation of cathodic dark- and photocurrents will increase towards more negative electrode potentials. In agreement with this concept, the onset of dark currents arising from the reduction of redox species such as Cu^{2+}, Fe^{3+}, Ru^{3+} and Ce^{4+} is observed at a potential negative from the flatband potential. The onset of photocurrents is seen to occur somewhat positive from the flatband potentials in the dark. Since positive photopotentials are observed it has to be assumed that illumination changes the flatband position of the electrode. Its behaviour is therefore still understandable. In the case of proton or water reduction, however, both dark and photocurrents are starting at potentials significantly more positive than the apparent flatband potential (0.2–0.3 and 0.65–0.75 V, respectively). In addition, the photopotential observed is quite small and can, together with the redox potential-dependent shift of the flatband potential, not be fitted into the systematic behaviour of other redox couples. Since cathodic dark and photocurrents starting positive to the 'flatband potential' are inconsistent with photoelectrochemical theory, a different phenomenon has to be taken into account.

A reasonable approach to this problem is to assume insertion of hydrogen into p-RuS_2. Like many other noble metals and metal oxides [37, 38] ruthenium and RuO_2 are known to insert hydrogen. Layer-type transition metal sulphide form insertion compounds of the type H_xMeS_2 (Me = transition metal) [38]. MoS_2, for example, forms an insertion compound with $x = 0.3$. Recently, evidence has also been given for hydrogen insertion into WSe_2 [39]. Also, a transition metal sulphide with pyrite structure, FeS_2, has been shown to incorporate and transport hydrogen [40]. RuS_2 itself is presently under study with respect to its ability to incorporate hydrogen [41]. It is therefore reasonable to attribute the abnormal apparent flatband behaviour observed with p-RuS_2 in presence of proton reduction to hydrogen insertion.

Let it be assumed that hydrogen insertion proceeds according to the reaction

$$H^+ + e \longrightarrow (H)_{ins} \tag{5}$$

Applying equilibrium thermodynamics the potential difference arising at the inserted electrode–electrolyte interface can be calculated by

$$V = V_0 + \frac{RT}{F} \ln \frac{a_{H^+}}{a_{(H)_{ins}}} \tag{6}$$

when a = activity.

It is justified to assume that insertion will proceed up to a saturation of the interface with inserted hydrogen which is equivalent to a constant activity. If this is considered, the formula for the potential drop in the interface reads

$$V = V_0' - 0.059 \text{ pH} \tag{7}$$

This corresponds to the observed pH-dependent shift of the apparent flatband potential. It can be concluded that proton insertion is compensating and preventing a significant energy band bending until the interface is saturated with inserted

hydrogen. Only then, i.e. at more negative potentials than the real flatband potential, the energy band bending can increase with increasingly negative electrode potential.

5. Conclusions

Crystals of p-RuS_2 grown in molten bismuth show quite unusual photoelectrochemical behaviour. The behaviour of the crystals is greatly influenced by the high number of surface states on the semiconductor surface. The presence of these surface states gives rise to a strong shift in the position of the bands. The shift occurs in the dark until the redox level of the electrolyte is reached. The capacity measurements reported here and previous photoelectrochemical measurements [11] support this hypothesis and indicate further complications due to hydrogen insertion.

Another important aspect of the photoelectrochemistry of this compound is the moderate blocking character of the Schottky barrier due to impurities lying in the forbidden gap. This fact, together with the variation of the position of the band edges, caused a metallic-like behaviour of the semiconductor in the dark. However, the shape of the dark characteristics reflects a rectifying property of the junction.

The presence of leakage currents crossing the barrier and the band shift are reflected in a photovoltage versus light intensity relationship which is linear up to illumination levels of some hundreds of $mW\,cm^{-2}$.

The question arises whether the impurities inside the band gap allowing the occurrence of forward dark currents and the surface states have the same physical origin or not. In the former case surface states should be caused by foreign atoms emerging at the surface. At present no experimental evidence exists. it is known, however, than n-type crystals grown with this procedure incorporate some quantity of bismuth [9]. Also, for p-RuS_2, ESCA measurements revealed the presence of about 4% of bismuth on the surface and inside the crystal [36]. This explains the dark conductivity of the barrier, but the origin of the photoelectrochemical behaviour of the crystals is not yet proved.

Deposition of metals onto the surface of p-RuS_2 crystals has been shown to improve the performance of the material for photo-assisted hydrogen evolution and dark oxygen reduction. For the hydrogen reaction platinum is the most effective of the metals investigated. The improvement is quite notable in the case of oxygen reduction in basic solution. Hence interest could arise in this kind of surface modification for practical purposes.

The mechanism of the catalytic effect of the metal particles on the semiconductor surface, its characteristics, limitations and durability are still unknown and can be an interesting topic for future investigation.

Acknowledgements

The authors are grateful to Dr N. Alonso Vante for performing LMIER measurements and to Dr H.-M. Kühne for helpful discussion. The assistance of Dr S. Fiechter in the crystal growth procedures is gratefully acknowledged.

References

[1] R. Guittard, R. Heindl, R. Parsons, A. M. Redon and H. Tributsch, *J. Electroanal. Chem.* **111** (1980) 401.
[2] R. Heindl, R. Parsons, A. M. Redon, H. Tributsch and J. Vigneron, *Surf. Sci.* **115** (1982) 91.
[3] H. Ezzaouia, R. Heindl. R. Parsons and H. Tributsch, *J. Electroanal. Chem.* **145** (1983) 279.
[4] *Idem, ibid.* **165** (1984) 155.
[5] H. Ezzaouia, R. Heindl and J. Loriers, *J. Mater. Sci. Letters* **3** (1984) 625.
[6] H.-M. Kühne and H. Tributsch, *J. Electrochem. Soc.* **130** (1983) 1448.
[7] *Idem, Ber. Bunsenges. Phys. Chem.* **88** (1984) 10.
[8] R. Bichsel, F. Levy and H. Berger, *J. Phys. C: Solid State Phys.* **17** (1984) L19
[9] H.-M. Kühne and H. Tributsch, *J. Electroanal. Chem.* **201** (1986) 263.
[10] H.-M. Kühne, PhD Thesis, Freie Universität Berlin (1985).
[11] S. Piazza, H.-M. Kühne and H. Tributsch, *J. Electroanal. Chem.* **196** (1985) 53.
[12] Y. Nakato S. Tonomura and H. Tsubomura, *Ber. Bunsenges. Phys. Chem.* **80** (1976) 1289.
[13] W. Kautek, J. Gobrecht and H. Gerischer, *ibid.* **84** (1980) 1034.
[14] A. Heller, E. Aharon-Shalom, W. A. Bonner and B. Miller, *J. Amer. Chem. Soc.* **104** (1982) 6942.
[15] M. Szlarczyk and J. O'M. Bockris, *ibid.* **88** (1984) 5241.
[16] H.-M. Kühne, W. Jaegermann and H. Tributsch, *Chem. Phys. Letters* **112** (1984) 160.
[17] J. P. Petit, N. Alonso Vante and P. Chartier, *J. Electroanal. Chem.* **157** (1983) 145.
[18] N. F. Mott, *Proc. Roy. Soc. A* **171** (1939) 27.
[19] W. Schottky, *Z. Phys.* **113** (1939) 367.

[20] J. W. Schultze and K. J. Vetter, *Ber. Bunsenges. Phys. Chem.* **75** (1971) 470.
[21] W. P. Gomes and F. Cardon, in 'Progress in Surface Science', Vol. 12, Pergamon Press (1982) pp. 155–216.
[22] W. Kautek and H. Gerischer, *Electrochim. Acta* **27** (1982) 1035.
[23] E. C. Dutoit, R. L. Van Meirhaeghe, F. Cardon and W. P. Gomes, *Ber. Bunsenges. Phys. Chem.* **79** (1975) 1206.
[24] M. D. Krotova, V. A. Myamlin and Yu. V. Pleskov, *Elektrokhimiya* **4** (1968) 579.
[25] S. J. Fonash, *J. Appl. Phys.* **54** (1983) 1966.
[26] H. Gerischer, *Surf. Sci.* **18** (1969) 97.
[27] J. J. Kelly and R. Memming, *J. Electrochem. Soc.* **129** (1982) 730.
[28] J. F. McCann and S. P. S. Badwal, *J. Electrochem. Soc.* **129** (1982) 551.
[29] J. P. Petit, N. Alonso Vante and P. Chartier, communication presented at the 'Journes d'Electrochemie '85', Florence 28–31 May 1985.
[30] J. Gobrecht and H. Gerischer, *Solar Energy Mater.* **2** (1979) 131.
[31] W. Kautek and H. Gerischer, *Electrochim. Acta* **27** (1982) 355.
[32] M. A. Lampert and P. Mark, 'Current Injection in Solids', Academic Press, New York (1970).
[33] S. Trasatti, *J. Electroanal. Chem.* **39** (1972) 163.
[34] H. Bala, *J. Phys. Chemie* **141** (1984) 91.
[35] B. Case, *Electrochim. Acta* **18** (1973) 293.
[36] W. Jaegermann, personal communication.
[37] G. Alfeld and J. Völkl (eds), 'Hydrogen in Metals', 1 & 2, Topics in Applied Physics, Vols 28, 29, Springer-Verlag, Berlin, Heidelberg, New York (1978).
[38] R. Schöllhorn, *Angew. Chemie* **92** (1980) 1015.
[39] A. J. McEvoy, *J. Electroanal. Chem.* **195** (1985) 207.
[40] S. M. Wilhelm, J. Vera and N. Hackerman, *J. Electrochem. Soc.* **130** (1983) 2129.
[41] H.-M. Kühne, R. A. Huggins and H. Tributsch, in preparation.